Stanford Exploration Project, Report 111, June 9, 2002, pages 149–156

Short Note

Reverse time migration in midpoint-offset coordinates

Biondo Biondi[1]

INTRODUCTION

Reverse-time migration (Baysal et al., 1984) has some potential advantages with respect to downward-continuation migration. It can migrate overturned and prismatic reflections even in the presence of strong lateral velocity variations (Biondi, 2002). It also models the amplitude of the transmitted wavefield more accurately than downward-continuation in the presence of sharp interfaces. However, it has the drawback of being computationally intensive. In particular, shot profile migration of overturned events can be extremely expensive because we need to pad the computational domain with a huge number of zero traces to assure that it includes the reflectors that generated the overturned events.

A similar problem of computational-domain size exists for shot profile migration by downward continuation. For marine data, an efficient solution to the problem is migration in midpoint-offset coordinate (Biondi and Palacharla, 1996). In the midpoint-offset domain the wavefield focuses towards zero offset, and thus we can drastically limit the length of the offset axes (at the limit we can eliminate the cross-line offset altogether by a common-azimuth approximation). It is thus natural to try to derive a reverse-time migration method that backward propagates the data in midpoint-offset coordinates.

In this paper, I derive an equation for backward propagating in time midpoint-offset domain data. The equation is derived from the Double Square Root equation. The proposed method successfully images non-overturned events. Unfortunately, the propagation equation has a singularity for horizontally traveling waves, thus the method does not seem capable of imaging overturned waves. The root of the problem is that the DSR implicitly assumes that the sources and the receivers are at the same depth level (or at least that their vertical offset is constant). This assumptions is clearly unfulfilled by finite-offset overturned events. I speculate that the assumption of null (constant) vertical offset between sources and receiver could be removed. In this case a midpoint-offset domain might be still computationally attractive because the reflected wavefield would still tend to focus towards zero offset as it is back-propagated in time.

[1]**email:** biondo@sep.stanford.edu

FROM DOWNWARD CONTINUATION TO TIME STEPPING

We would like to propagate the recorded wavefield backward in time instead of downward into the Earth, but we also would like to preserve the computational advantages of propagating the recorded wavefield in midpoint-offset coordinates. The advantage of the midpoint-offset coordinates derives from the focusing of the reflected wavefield towards zero offset as it approaches the reflector. The wavefield focuses towards zero-offset during downward continuation because we are essentially datuming the whole data set to an increasingly deeper level in the Earth. It is thus reasonable to start our derivation from the double square root (DSR) equation, that is the main tool for datuming prestack data. As we will see later, this choice of a starting point limits the usefulness of the final result.

The DSR equation in the frequency-wavenumber domain is

$$k_z = \sqrt{\omega^2 s(\mathbf{s},z)^2 - k_{x_s}^2} + \sqrt{\omega^2 s(\mathbf{g},z)^2 - k_{x_g}^2}, \tag{1}$$

where ω is the temporal frequency, k_{x_s} and k_{x_g} are respectively the wavenumber associated to the source and receiver locations, and $s(\mathbf{s},z)$ and $s(\mathbf{g},z)$ are the slowness at the source and receiver locations. We first start by rewriting the DSR in terms of midpoint x_m and half offset x_h as

$$k_z = \sqrt{\omega^2 s(\mathbf{s},z)^2 - \frac{\left(k_{x_m} - k_{x_h}\right)^2}{4}} + \sqrt{\omega^2 s(\mathbf{g},z)^2 - \frac{\left(k_{x_m} + k_{x_h}\right)^2}{4}}, \tag{2}$$

where k_{x_m} and k_{x_h} are respectively the wavenumber associated to the midpoint x_m and the half-offset x_h.

Then, to obtain a time marching equation, we first square equation (2) twice and rearrange the terms into:

$$\omega^4 \Delta_s + 2\omega^2 \left(\Delta_s k_{x_m} k_{x_h} - \Sigma_s k_z^2\right) + k_z^4 + k_z^2 \left(k_{x_m}^2 + k_{x_h}^2\right) + k_{x_m}^2 k_{x_h}^2 = 0, \tag{3}$$

where

$$\Delta_s = s(\mathbf{s},z)^2 - s(\mathbf{g},z)^2 \tag{4}$$

$$\Sigma_s = s(\mathbf{s},z)^2 + s(\mathbf{g},z)^2 \tag{5}$$

Equation (3) is a second order equation in ω^2. It has another solution in addition to the desired one. It can be greatly simplified by assuming $\Delta_s \approx 0$. Then equation (3) can be rewritten as

$$\omega^2 = \frac{1}{2\Sigma_s}\left(k_z^2 + k_{x_m}^2 + k_{x_h}^2 + \frac{k_{x_m}^2 k_{x_h}^2}{k_z^2}\right). \tag{6}$$

This is the basic equation solved for the numerical examples shown in this paper. Notice that when k_{x_h} is equal to zero, equation (6) degenerates to the well-known equation used for reverse-time migration of zero-offset data (Baysal et al., 1984).

There are few alternatives on how to solve equation (6) numerically. The simplest one is to use finite-differences for approximating the time derivative, and Fourier transforms for evaluating the spatial-derivative operators. Because the slowness term Σ_s is outside the parentheses in equation (6), using Fourier transforms does not preclude the use of a spatially variable slowness field. Strong lateral velocity variations would cause problems because of the approximations needed to go from equation (3) to equation (6), not because of the numerical scheme used to solve equation (6).

The time marching scheme that I used can be summarized as;

$$\frac{P_{t-\Delta t} - 2P_t + P_{t+\Delta t}}{\Delta t^2} = \frac{1}{2\Sigma_s} \text{FFT}^{-1} \left(k_z^2 + k_{x_m}^2 + k_{x_h}^2 + \frac{k_{x_m}^2 k_{x_h}^2}{k_z^2} \right) \text{FFT} \;\; P. \tag{7}$$

Using a Fourier method to evaluate the spatial-derivative operators, makes it easy to handle the real limitation of equation (6); that is, the presence of the vertical wavenumber k_z at the denominator. Waves propagating horizontally have an effective infinite velocity, making a finite-difference solution unstable, no matter how small the extrapolation time step. Unfortunately, this is a major obstacle for migrating overturned events, which is one of the main goals for developing a reverse time migration in midpoint-offset coordinates. The problem exists only for finite offset data ($k_{x_h} \neq 0$). In retrospective, the occurrence of problems for waves that overturn at finite offset should not be surprising. Equation (6) was derived from the DSR that cannot model data for which the source leg overturns at different depth than the receiver leg.

For non-overturning events the problem can be sidestepped. The spatial wavenumbers are related to the reflector geological dip angle γ and the aperture angle α by the relationship

$$\frac{k_{x_m}^2 k_{x_h}^2}{k_z^2} = \tan\alpha \tan\gamma, \tag{8}$$

By simple trigonometry is also possible to show that for non-overturned events

$$\frac{k_{x_m}^2 k_{x_h}^2}{k_z^2} a \leq 1. \tag{9}$$

In the Fourier domain it is straightforward to include condition (9) in the time-marching algorithm and thus to avoid instability without suppressing reflected energy.

Stronger lateral velocity variations?

The numerical scheme described by equation (7) can probably handle some amount of lateral velocity variations, but it would be inaccurate for more complex velocity functions. In the derivation presented in the previous section there is no assumption of mild lateral velocity variations up to equation (3). The problem with equation (3) is that it is fourth order in time. In addition to the desired solution it has another solution that can generate artifacts and cause instability. Therefore, a direct solution by finite-differences would encounter problems with

the spurious solution. Alkhalifah (1998) describes a similar problem when solving an acoustic wave equation for anisotropic media.

However, it is fairly straightforward to derive an approximation to equation (3) that is more accurate than equation (6). Equation (3) can be easily solved for ω^2 because it contains only the even powers of ω. We can then approximate the square root that appears in the formal solution for ω^2 as

$$\sqrt{1-\frac{\Delta_s\left[k_z^4+k_z^2\left(k_{x_m}^2+k_{x_h}^2\right)+k_{x_m}^2k_{x_h}^2\right]}{\left(\Delta_s k_{x_m}k_{x_h}-\Sigma_s k_z^2\right)^2}}\approx 1-\frac{\Delta_s\left[k_z^4+k_z^2\left(k_{x_m}^2+k_{x_h}^2\right)+k_{x_m}^2k_{x_h}^2\right]}{2\left(\Delta_s k_{x_m}k_{x_h}-\Sigma_s k_z^2\right)^2}. \tag{10}$$

The useful solution of equation (3) can then be approximated as

$$\omega^2=\frac{1}{2\left(\Sigma_s-\Delta_s k_{x_m}k_{x_h}\right)}\left(k_z^2+k_{x_m}^2+k_{x_h}^2+\frac{k_{x_m}^2k_{x_h}^2}{k_z^2}\right). \tag{11}$$

Equation (11) degenerates to equation (6) when Δ_s is zero. It is more accurate than Equation (6) for Δ_s different than zero, but it is likely to break down for strong lateral velocity variations.

Equation (11) shares with equation (6) the fundamental problem of instability for horizontally propagating waves. Therefore, I have not implemented a numerical scheme to solve equation (11) yet. However, it is possible to define a mixed implicit-explicit method to solve equation (11), similar to the one proposed by Klíe and Toro (2001) to solve Alkhalifah's acoustic wave equation for anisotropic media.

Imaging principle

One of the advantages of the choice of the midpoint-offset coordinate to migrate the data is that the imaging step is both straightforward and inexpensive. There is no need to crosscorrelate and shift wavefields, as for shot-profile reverse-time migration (Biondi, 2002).

The equivalent of the "stacked" image is obtained by selecting the propagated wavefield at zero time and zero offset; that is

$$I\left(z,x_m\right)=P\left(t=0,z,x_m,x_h=0\right) \tag{12}$$

The offset-domain Common Image Gathers (CIG) are obtained by simply selecting the propagated wavefield at zero time; that is

$$I\left(z,x_m,x_h\right)=P\left(t=0,z,x_m,x_h\right). \tag{13}$$

EXAMPLES OF REVERSE TIME MIGRATION OF A SYNTHETIC DATA SET

To illustrate the use of the proposed method to image seismic data by reverse-time migration, I migrated the same simple synthetic data set (with a dipping and a flat layer) that I used in Biondi (2002). Since the data were modeled in shot gathers, I sorted the data set in midpoint-offset coordinates before migration. As in the other paper, I migrated the data with a constant velocity to avoid artifacts caused by velocity discontinuities in the migration velocity. Therefore, the deeper reflector is slightly undermigrated.

Figure 1 is the equivalent of the "stacked" image, obtained by applying equation (12). The dipping reflector is well imaged within the range that is illuminated by the shots. The flat reflector is slightly undermigrated, as discussed above. The quality of the image is comparable to the quality of the image obtained by shot-profile migration using the same data.

Figure 2 shows on the left the offset-domain CIG (a) and on the right the angle-domain CIG (b). The offset domain CIG was obtained by applying equation (13), and the angle-domain CIG was obtained by applying the offset-to-angle transformation presented in Sava et al. (2001). The CIGs are located at a surface location where both reflectors are well illuminated (1,410 m). As expected the image is well focused at zero-offset in the panel on the left and the events are flat in the panel on the right.

As for shot-profile migration, the CIGs obtained by midpoint-offset reverse-time migration can be easily used for velocity updating. To illustrate this capability, I have migrated the same data set with a lower velocity (.909 km/s). Figure 3 is the "stacked" image obtained using the lower velocity. Both reflectors are undermigrated and shifted upward.

Figure 4 shows on the left the offset-domain CIG (a) and on the right the angle-domain CIG (b). Now in the panel on the left, the energy is not well focused at zero offset but is spread over an hyperbolic trajectory centered at zero offset. The corresponding angle-domain CIG (ADCIG) (right) shows the characteristic smile typical of undermigrated ADCIG. The velocity information contained in the panel on the right can be easily used for velocity updating and tomographic inversion in a similar way as the ADCIG obtained by downward-continuation migrations are used (Clapp and Biondi, 2000; Clapp, 2001).

CONCLUSIONS

I explore the possibility of imaging prestack data by reverse-time migration in the midpoint-offset domain. The method that I derive successfully imaged a simple synthetic data set. However, it is not capable of migrating correctly overturned events, which is one of the main goals of the effort. This limitation originates from the limitations of the starting point of my derivation; that is, the Double Square Root equation. The DSR assumes a null (constant) vertical offset between source and receivers. The choice of a more general starting point might lead to a useful migration method.

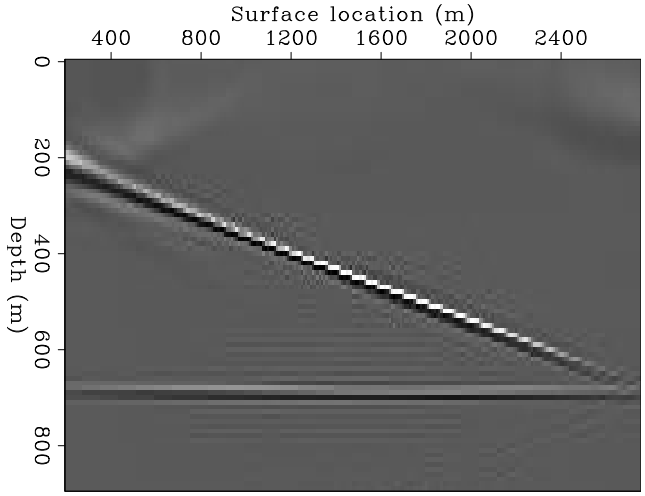

Figure 1: Image of the synthetic data set with the correct velocity function. biondo1-MidOff-Image-dip [CR]

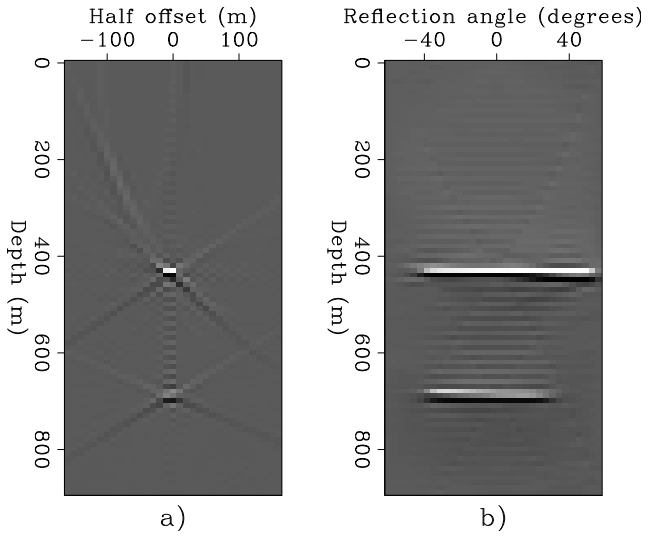

Figure 2: Offset-domain CIG (left a)) and angle-domain CIG (right b)) corresponding to the image in Figure 1. Notice the focusing at zero offset in a), and the flatness of the moveout in b). biondo1-MidOff-Cig-Ang-dip [CR]

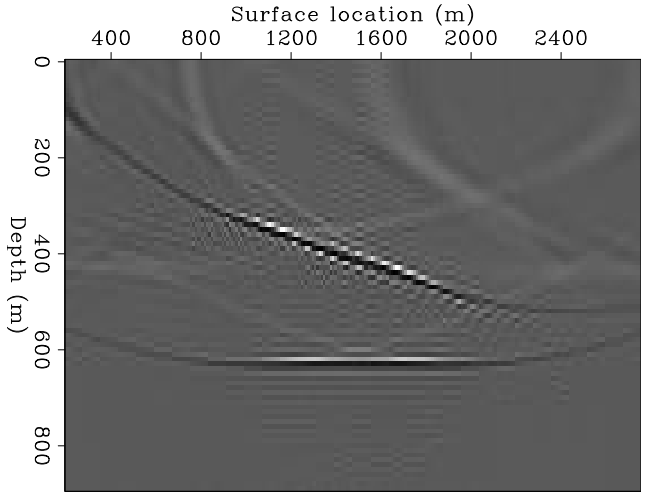

Figure 3: Image of the synthetic data set with the incorrect velocity function. biondo1-MidOff-Image-dip-slow [CR]

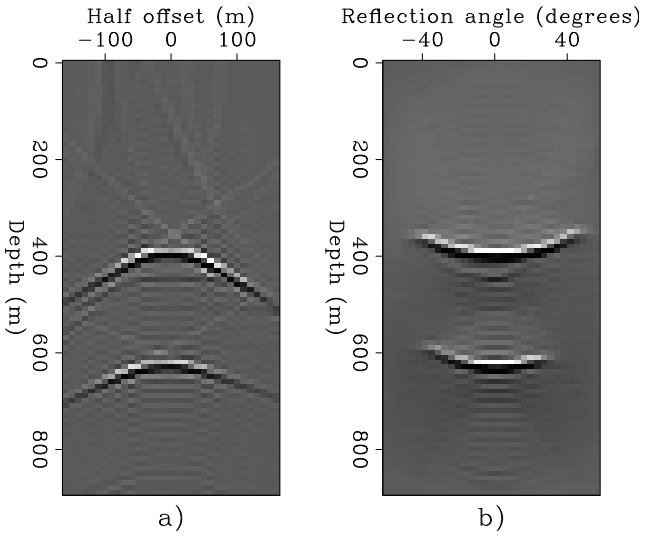

Figure 4: Offset-domain CIG (left) and angle-domain CIG (right) corresponding to the image in Figure 3. Notice the lack of focusing at zero offset in a), and the smile in b). biondo1-MidOff-Cig-Ang-dip-slow [CR]

REFERENCES

Alkhalifah, T., 1998, An acoustic wave equation for anisotropic media: 68th Ann. Internat. Meeting, Soc. Expl. Geophys., Expanded Abstracts, 1913–1916.

Baysal, E., Kosloff, D. D., and Sherwood, J. W. C., 1984, A two-way nonreflecting wave equation: Geophysics, **49**, no. 02, 132–141.

Biondi, B., and Palacharla, G., 1996, 3-D prestack migration of common-azimuth data: Geophysics, **61**, no. 6, 1822–1832.

Biondi, B., 2002, Prestack imaging of overturned and prismatic reflections by reverse time migration: SEP–**111**, 123–139.

Clapp, R., and Biondi, B., 2000, Tau domain migration velocity analysis using angle CRP gathers and geologic constrains:, *in* 70th Ann. Internat. Mtg Soc. of Expl. Geophys., 926–929.

Clapp, R. G., 2001, Geologically constrained migration velocity analysis: Ph.D. thesis, Stanford University.

Klíe, H., and Toro, W., 2001, A new acoustic wave equation for modeling in anisotropic media: 71st Ann. Internat. Mtg., Soc. Expl. Geophys., Expanded Abstracts, 1171–1174.

Sava, P., Biondi, B., and Fomel, S., 2001, Amplitude-preserved common image gathers by wave-equation migration: 71st Ann. Internat. Mtg., Soc. Expl. Geophys., Expanded Abstracts, 296–299.